# Ultrastructure of Interactions
# Between Cassava and *Xanthomonas campestris* pv. *manihotis*:
# Cytochemistry of Cellulose and Pectin Degradation in a Susceptible Cultivar

B. Boher, K. Kpemoua, M. Nicole, J. Luisetti, and J. P. Geiger

First, second, third, and fifth authors: ORSTOM, Laboratoire de Phytopathologie, B.P. 5045, 34032 Montpellier, France; fourth author: INRA, Station de Pathologie Végétale et Phytobactériologie, B.P. 57, 49071 Beaucouzé Cedex, France.

## ABSTRACT

Boher, B., Kpemoua, K., Nicole, M., Luisetti, J., and Geiger, J. P. 1995. Ultrastructure of interactions between cassava and *Xanthomonas campestris* pv. *manihotis*: Cytochemistry of cellulose and pectin degradation in a susceptible cultivar. Phytopathology 85:777-788.

A cytochemical investigation was carried out on the development of an aggressive strain of *Xanthomonas campestris* pv. *manihotis*, responsible for the cassava bacterial blight, to gain better insights into molecular and cellular mechanisms involved in leaf cell wall degradation by this pathogen. The use of anti-pectin monoclonal antibodies revealed that the plant middle lamellae were damaged during the infection process, from the epiphytic stage on the leaf surface to invasion of vascular bundles. In parallel, application of a β-1,4-exoglucanase-gold probe to healthy and infected tissues indicated that primary and secondary cell walls were also altered. Quantitation of gold labeling confirmed that pectin was more severely degraded than cellulose. Accumulation of pectinlike compounds was also detected in occluded infected vessels. Bacterial-surrounding sheaths, which were routinely seen during pathogenesis early after leaf inoculation, had a dense or loosened fibrillar appearance and were differentiated from the pathogen cell wall. Close association occurred between extracellular fibrils and leaf cell walls, both at early and advanced stages of wall degradation. Bacterial extracellular sheaths were often seen deep in host cell walls, sometimes enclosing residual plant cell wall fragments. Our cytochemical data demonstrated that cell wall degradation of cassava by *Xanthomonas campestris* pv. *manihotis* plays an important role in host tissue colonization. It is also suggested that bacterial extracellular sheaths are involved in plant cell surface degradation.

Cassava, *Manihot esculenta* Crantz, is one of the most important food crops in intertropical Africa. It belongs to the Euphorbiaceae, a well-known laticifer family in the plant world. Among pests and diseases that may reduce the production of both tubers and planting material, the cassava bacterial blight, caused by *Xanthomonas campestris* pv. *manihotis* (Berthet and Bondar) Dye (*XCM*), is one of the major damaging diseases. Symptoms include angular leaf spot, blight, wilting, and stem die-back after systemic infection.

Previous histopathological investigations of *Xanthomonas*-infected plant tissues have shown that the infection process starts with the epiphytic activity of the pathogen on leaves (11). This first stage of infection contributes to a buildup of inoculum sufficient to increase significantly the probability of leaf penetration through stomatal apertures and wounds (47). The multiplication of the pathogen within the mesophyll and bacterial exopolysaccharides (EPS) production results in swelling of substomatal cavities and intercellular spaces, contributing to water soaking (1,5). At this stage, host cells display cellular alterations such as middle lamellae dissolution (1,33), invagination of the plasmalemma (27,33), accumulation of vesicles in periplasmic spaces (27), modification of cytoplasm (which becomes clumped and electron-dense), and disorganization of chloroplasts (7). Some *X. campestris* pathovars then colonize xylem vessels of leaves, spreading upward and downward from the initial point of entry and extending to all parts of the plant (7,16).

Previous biochemical studies pointed out the production in vitro of plant cell wall–degrading enzymes by *X. campestris* patho-vars (13,26). Pectinases (10,12,31) and polygalacturonase (13) were demonstrated to be active enzymes occuring in *Xanthomonas*, but their roles in pathogenicity were not clearly established. Nevertheless, molecular cloning of polygalacturonase lyase genes indicated that virulence of mutants was significantly reduced (15). Plant bacterial pathogens, including *Pseudomonas* (29), *Erwinia* (6), and *Clavibacter* (4) species were also known to alter plant cell wall polymers (17). Cellulase (20,31), endoglucanase (12), and xylanase (42) produced by *Xanthomonas* species may have the potential capacity for degrading host cellulose and hemicellulose, but virulence of cellulase-deficient mutants of *X. c.* pv. *campestris* was not significantly less than that of the wild-type strain (21). Alteration of lignified secondary cell walls of xylem vessels indicated that *Xanthomonas* depolymerized lignin in vitro (17,30).

To our knowledge, little is known about in situ modifications of the plant cell wall structural polymers following an infection by *Xanthomonas* species. Ultrastructural features of host colonization have been reported, but no detailed analysis of plant cell wall degradation has been presented. The apparent release of fibrillar material from damaged plant cell walls during colonization of leaves by the pathogen has already been described (9,48), but there was no evidence that this material was of host origin. In this respect, a cytochemical investigation of plant cell wall degradation was of interest in characterizing host wall fragments within EPS produced by the bacteria during leaf colonization.

The present study was undertaken to gain greater insight into molecular and cellular mechanisms involved in leaf cell wall degradation of a susceptible cassava cultivar during the infection process of an aggressive wild-type strain of *XCM*. To study the distribution of cellulose and pectin in cell walls and middle lamellae, particular attention was paid to the cytolocalization of β-1,4-glucans and epitopes of pectic components by using gold-conjugated probes.

## MATERIALS AND METHODS

**Plant material.** A susceptible cassava cultivar, *Manihot esculenta* Crantz var. *Fetonegbodji,* was rendered virus free by thermotherapy and meristem regeneration and then multiplied in culture flasks (28). This material was used for artificial infection.

**Bacterial strains.** The aggressive *XCM* strain X27 was isolated from naturally infected cassava in Togo. It was routinely grown for 36 h at 30 C on 5% yeast extract, 5% peptone, 5% glucose, and 15% agar (Difco, Detroit) in petri dishes. For inoculum preparation, the culture was washed two times in distilled water and collected by centifugation at 11,000 g for 10 min. The pellet was resuspended in 0.05% Tween 80 in distilled water and photometrically adjusted to $10^8$ cfu per milliter.

**Artificial infection of leaves.** The lower side of fully expanded leaves from 6-wk-old in vitro plants was infected by spraying with the bacterial suspension (airbrush, PAASCHE, type VLS7440, Hardwood Heights, IL) or water as a control. Healthy and infected plants were incubated at $27.5\pm0.5$ C, 12 h light/dark regime (fluorescent, cool white, 40 W) in controlled climate chamber (85% RH). For microscopy, leaves were taken 0.5, 1, 2, 3, 5, 7, and 9 days after inoculation. Since all stages of the infection process occurred at each time of sampling, descriptions are provided according to the spatial localization of *XCM* in infected leaf tissues.

**Tissue processing.** Fragments of inoculated and healthy leaf tissues were fixed for 4 h in a mixed solution of 2.5% glutaraldehyde and 4% paraformaldehyde in 0.1 M sodium cacodylate buffer (pH 7.2). For immunocytochemistry of the bacterial cell wall, half samples were rinsed in buffer, dehydrated in alcohol, and embedded in LR White (London Resin Co., TAAB, Reading, England) medium grade. For conventional ultrastructure and cytochemistry, the remaining samples were postfixed for 1 h in 1% osmium tetroxide ($OsO_4$) in water, dehydrated in alcohol, and embedded in Epon 812 resin (TAAB, Reading, England). Selected material was sectioned with a diamond knife on a Reichert Ultracut E microtome, and sections were collected on nickel grids and processed for labeling studies. The grids were examined using a Jeol 100 electron microscope (LPRC-CIRAD) operating at 80 kV.

**Cytochemistry.** The exoglucanase, a $\beta$-(1-4)-D glucan cellobiohydrolase (E.C. 3.2.1.91), used in this study was purified in a five-step procedure from a cellulase produced by the cellulolytic fungus *Trichoderma harzianum* (37). Optimal activity of the enzyme was estimated to be at pH 5.0–5.6.

Colloidal gold (Sigma, St. Louis, MO) with particles averaging 15 nm in diameter was prepared according to Frens (19). Ten ml of the gold suspension, adjusted to pH 9.0 (isoelectric point of the enzyme) with 0.2 M $K_2CO_3$, was added to 1 mg of purified exoglucanase dissolved in 0.2 M phosphate-buffered saline (PBS), pH 7.4. The mixture was centrifuged at 25,000 g with a Ti 50 rotor for 45 min. The red mobile pellet was recovered in 0.5 ml of PBS, pH 6.0, containing 0.02% (w/v) of polyethylene glycol (PEG 20,000).

Sections of infected and healthy leaf samples were first floated on a drop of PBS-PEG, pH 6.0, then incubated in a moist chamber on a drop of the enzyme-gold complex for 30 min at room temperature. They were then thoroughly washed with PBS, pH 7.4, rinsed with distilled water, and finally contrasted with uranyl acetate and lead citrate before examination. Specificity of labeling was assessed by means of the following control tests (37): incubation with the exoglucanase-gold complex to which 2 mg ml$^{-1}$ of $\beta$-(1-4)-D-glucans were previously added, and incubation of noninoculated healthy plants (3).

**Immunocytochemistry.** Monoclonal antibodies (JIM 5) raised against un-esterified epitopes of pectin were used to visualize galacturonic acid–containing molecules in infected and healthy samples. Immunogold localization of pectin was performed as previously described by Knox et al (32). Briefly, sections were first incubated for 2 h at 37 C on a drop containing primary antibodies, and then 30 min at 37 C on a drop of a gold-labeled (10nm) goat anti-rat antibodies (GAR 10, Biocell Research Lab., Cardiff, UK) diluted 1:20 in Tris/HCl-BSA-Tween 20.

A polyclonal antiserum was raised in Fauve de Bourgogne rabbits periodically immunized over a 3-mo period through four intracutaneous injections (7, 21, and 37 days after the first injection) of heat-killed washed whole bacterial cells. After each injection, 5 ml of serum was collected from rabbits and tested by immunofluorescence. Ultrathin sections of material not treated with osmium were pretreated with 0.1 M glycine, pH 7.1, in PBS

TABLE 1. Density of labeling obtained with gold-complexed exoglucanase over walls of healthy and infected leaf cells during infection process[a]

|  | Healthy tissues | Infected tissues | $\chi^2$ | P |  | Control[b] |
|---|---|---|---|---|---|---|
| Parenchyma primary wall[c] | $461 \pm 82$ | $122 \pm 107$ | 5.0 | <0.05 | S[d] | 0 |
| Xylem primary wall | $311 \pm 100$ | $180 \pm 86$ | 2.7 | <0.1 | S | 0 |
| Xylem secondary wall | $195 \pm 87$ | $193 \pm 212$ | 1.8 | >0.1 | NS | 0 |
| Xylem vessel lumen | 0 | $18 \pm 21$ | ... | ... | ... | 0 |
| Parenchyma intercellular spaces[e] | $9 \pm 17$ | $59 \pm 59$ | ... | ... | ... | 0 |
| Parenchyma background | $14 \pm 16$ | $10 \pm 18$ | ... | ... | ... | 0 |
| Xylem background | $2 \pm 4$ | $4 \pm 6$ | ... | ... | ... | 0 |

[a] Data are expressed as means of 8–15 fields.
[b] Gold probe was previously incubated with an excess of barley glucans.
[c] Including cell walls of both the upper and lower parenchyma.
[d] S = significant; NS = not significant.
[e] In infected tissues, intercellular spaces are filled with bacterial EPS.

TABLE 2. Density of labeling obtained with anti-pectin antibodies over middle lamellae of healthy and infected leaf cells during infection process[a]

|  | Healthy tissues | Infected tissues | $\chi^2$ | P |  | Control[b] |
|---|---|---|---|---|---|---|
| Parenchyma middle lamella[c] | $417 \pm 71$ | $118 \pm 56$ | 5.8 | <0.05 | S[d] | $19 \pm 16$ |
| Xylem middle lamella | $263 \pm 42$ | $94 \pm 96$ | 7.7 | <0.01 | S | $19 \pm 16$ |
| Xylem vessel lumen | $9 \pm 18$ | $26 \pm 26$ | ... | ... | ... | 0 |
| Parenchyma intercellular spaces[e] | $13 \pm 26$ | $30 \pm 45$ | ... | ... | ... | 0 |
| Parenchyma background | $4 \pm 12$ | $7 \pm 12$ | ... | ... | ... | 0 |
| Xylem background | $18 \pm 30$ | $18 \pm 27$ | ... | ... | ... | 0 |

[a] Data are expressed as means of 8–15 fields.
[b] Anti-pectin antibody was previously incubated with an excess of polygalacturonic acid.
[c] Including middle lamellae of both the upper and lower parenchyma.
[d] Significant.
[e] In infected tissues, intercellular spaces are filled with bacterial EPS.

to quench aldehyde groups induced during fixation. Sections were then incubated for 10 min at room temperature on a drop of normal goat serum (1:20) in PBS. Sections were then incubated for 2 h at 25 C with the primary antiserum diluted 1:200 and then for 1 h at room temperature with a gold-labeled (15nm) anti-rabbit immunoglobulin G conjugate (goat anti-rabbit GAR15, BioCell Research Laboratories, Cardiff, UK) diluted 1:20 in Tris/HCl-BSA-Tween 20.

Monoclonal antibody XB3 (IgMk) raised against xanthan from *X. c.* pv. *campestris* strain 644 (22), was used for labeling *XCM* EPS. The plant sections were incubated overnight at 4 C in a drop of the primary antibody (diluted 1:1,000) and treated as decribed above with a gold-labeled (15 nm) goat antimouse secondary antibody (GAm 15, Biocell Research lab., Cardiff, UK) diluted 1:20 in Tris/HCl-BSA-Tween 20.

Controls used for immunolabeling of healthy and infected leaves
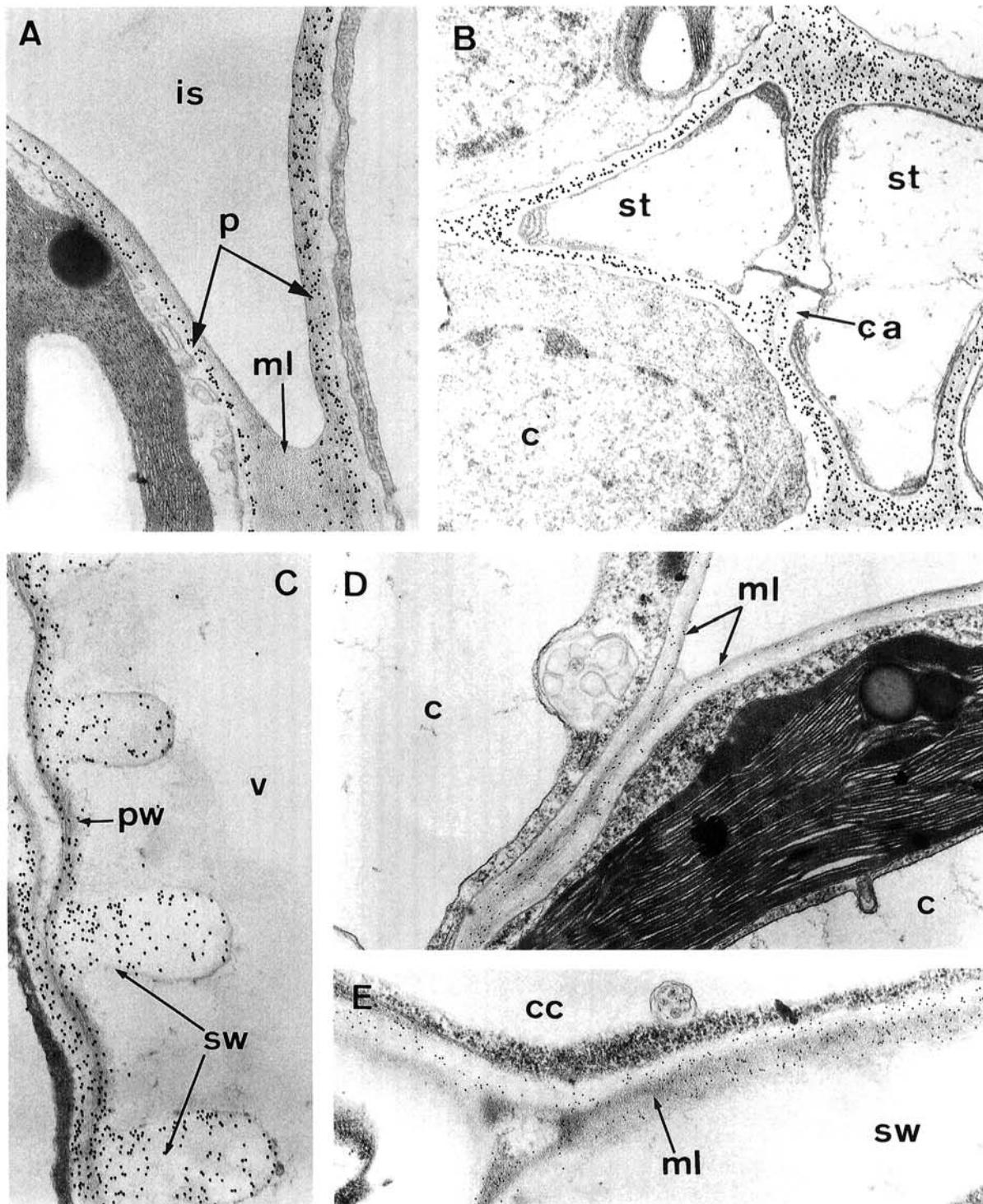


**Fig. 1. A–C,** TEM micrographs of healthy cassava leaves fixed with glutaraldehyde and osmium tetroxide. Sections treated with exoglucanase-gold complex. **A,** Walls (p) of mesophyll cells at lower part of leaf are evenly labeled; few gold particles are seen over middle lamella (ml). Intercellular space (is) is devoid of any labeling. (×26,600). **B,** In vascular stele, walls of phloem sieve tubes (st) and parenchyma cells (c) display regular labeling. No gold particles are noticed over callose deposition (ca) on sieve plates. (×22,400). **C,** Gold particles are present over primary (pw) and secondary (sw) walls of xylem vessel (v). (×26,600). **D and E,** TEM micrographs of healthy cassava leaves fixed with glutaraldehyde and osmium tetroxide. Sections treated with JIM 5 anti-pectin antibodies. **D,** Gold particles are evenly distributed over middle lamella (ml) of two mesophyll cells (c) of upper part of leaf. Few gold particles visible over primary walls. (×26,600). **E,** Regular labeling is present over middle lamella (ml) between xylem vessels and companion cell (cc). Secondary cell walls (sw) are devoid of significant labeling. (×26,600).
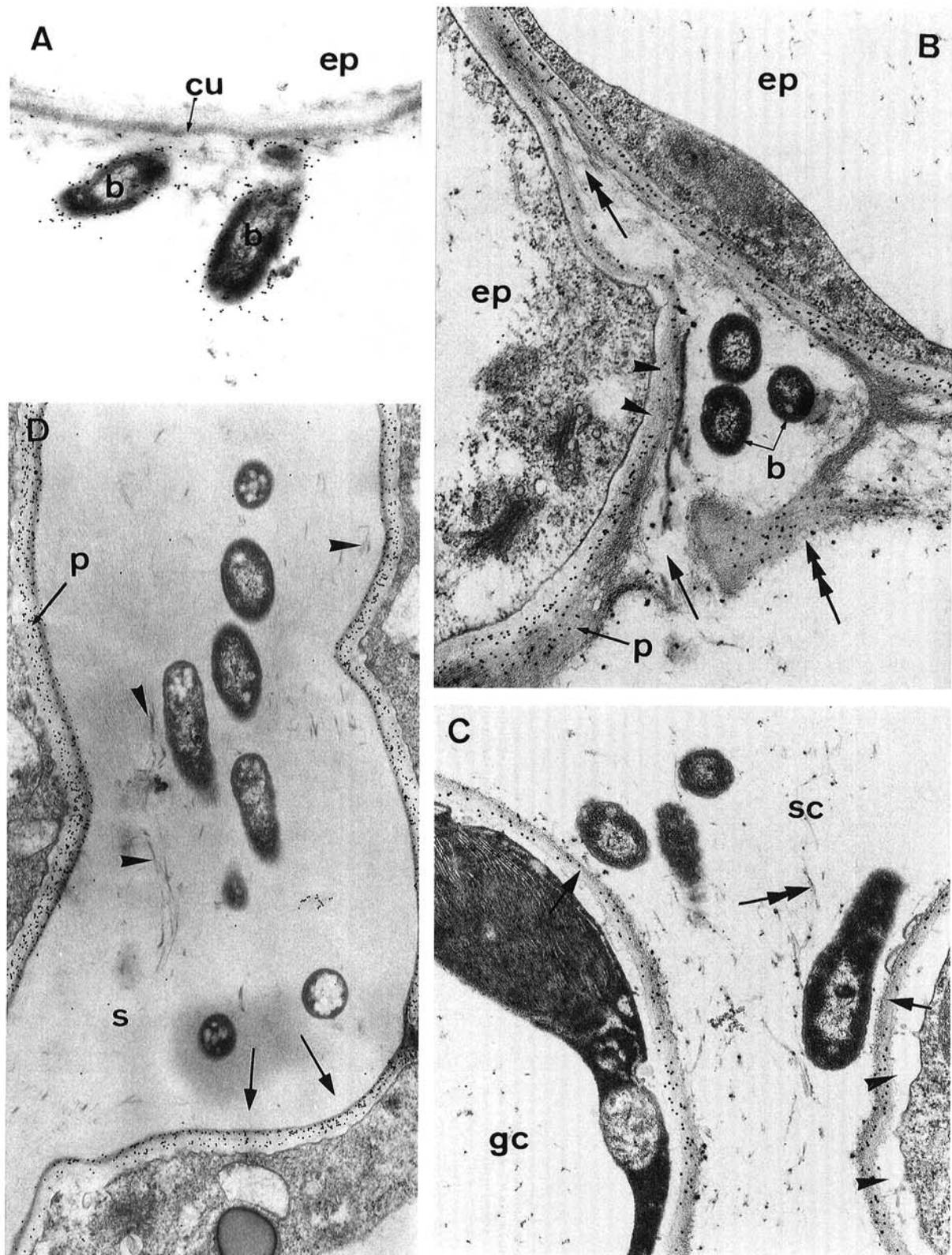
**Fig. 2.** TEM micrographs of infected cassava leaves by *Xanthommnas campestris* pv. *manihotis* (*XCM*). **A,** TEM micrograph of cassava leaves infected by *XCM* fixed with glutaraldehyde alone, 1 day after infection (dai). Infected leaves incubated with anti-*XCM* antibodies. Gold particles are located close to bacterial (b) cell walls; a few are also seen over fibrillar material that adheres to epidermal (ep) cell cuticle (cu). (×23,000). **B–D,** TEM micrographs of cassava leaves infected by *XCM* fixed with glutaraldehyde and osmium tetroxide, 2 dai. Sections treated with exoglucanase-gold complex. **B,** At lower leaf surface, bacterial cells (b) are located between two epidermal cells (ep). Disruption (arrow) of wall (p) occurs in vicinity of pathogen. Labeling of wall (p) close to bacterial cells is reduced (arrowheads). A portion of uneven labeled wall (triple arrow) is detached from the main cell frame. Degradation (double arrow) of middle lamella (ml) is also observed. (×23,100). **C,** In substomatal cavity (sc), bacteria are in close contact with primary cell wall. Reduction of labeling is visible at these sites (arrows). Cytoplasm of guard cells (gc) is retracted (arrowheads). No gold particles are seen over strands of the dense material within bacteria-surrounding sheath (double arrows). (×22,400). **D,** Extracellular sheath (s) fills intercellular space of spongy parenchyma, resulting in distortion of plant cells (arrows). Strands occur within sheath (arrowheads). On this micrograph, no significant decrease of labeling is observed over the distorted primary host cell wall (p). (×18,000).

included samples incubated either with antibodies/antiserum previously absorbed with the corresponding antigen, or with pre-immune rat, rabbit, or mouse serum (respectively) instead of the primary antiserum.

**Quantitation of labeling.** The density of labeling (D) over sections of healthy and leaf samples was compared by determining the number of gold particles per $\mu m^2 \pm$ standard error. The density of labeling was calculated as D = number of gold particles (Ns) / area surface (Sa). Densities were determined by counting the number of gold particles over specified cell areas on 8–15 micro-photographs taken randomly from serial sections made on each of five blocks from infected cassava leaves and controls. The average gold particle densities for healthy and infected tissues were compared using the Kruskal-Wallis rank test, which is based on a statistic distributed as chi-square with one degree of freedom. The value of the statistic and the corresponding $P$ value are given in Tables 1 and 2.

## RESULTS

**Labeling pattern observed in healthy leaves.** Following incuba-tion of ultrathin sections of noninoculated leaf tissues with the exoglucanase-gold complex, an intense and regular labeling occurred over cell walls of most tissues. All other structures, including organelles, cytoplasm, and plasma membrane, were free of any significant labeling. Walls of parenchyma cells were evenly labeled (Fig. 1A). Very few gold particles were found to be associated with the middle lamella adjacent to parenchyma cells. A heavy deposition of gold particles occurred over primary walls of phloem cells such as sieve tubes or associated parenchyma cells (Fig. 1B). In the xylem, primary and secondary vessel cell walls were strongly labeled (Fig. 1C), whereas the electron-opaque middle lamella and pit membranes were slightly labeled.

Incubation of ultrathin sections of noninoculated leaf tissues with monoclonal antibodies raised against epitopes of pectin (JIM 5) led to a regular labeling over middle lamellae and primary walls of parenchyma (Fig. 1D) and phloem tissues. Similarly, gold particles were abundant over middle lamellae of the xylem, whereas no labeling was observed over the secondary cell walls (Fig. 1E).

In all controls, including incubation of sections with the exo-glucanase-gold complex or with the primary antibody to which was previously added an excess of $\beta$-1,4-glucans from barley or pectin, respectively, no significant labeling was observed (Tables 1 and 2).

**Labeling pattern for cellulose observed in infected leaves.** Description of data will be made according to the spatial locali-zation of *XCM* in infected leaf tissues. On the lower leaf surface, 24 h after infection, bacteria adhered to the cuticle. At this stage, a fibrillar-like material that was weakly labeled with anti-*XCM* polyclonal antibodies (Fig. 2A) was found to be associated with the plant surface. Following incubation with the exoglucanase-gold complex for localizing $\beta$-1,4-D-glucans, gold particles were mainly detected over walls of epidermal cells. Bacteria located at the leaf surface between two epidermal cells were associated with host wall degradation (Fig. 2B). Reduction of labeling was observed over cell walls close to the pathogen (Fig. 2B); portions of labeled cell walls were detached from the main cell framework (Fig. 2B).

In substomatal cavities (Fig. 2C) and between mesophyl cells (Fig. 2D), 48 h after inoculation, numerous bacterial cells were seen close to host cell walls. Labeling over plant walls was signifi-cantly reduced (Fig. 2C) compared with cell walls in healthy leaves (Table 1). Retraction of host cell cytoplasm occurred when bacteria were located in their vicinity. No gold particles were detected over the fibrillar material, or sheath, that surrounded the bacterial cells (Fig. 2C,D). Strands of more dense structures enclosed in this extracellular sheath were also devoid of significant labeling (Figs. 2C,D and 3A,B,D). In the spongy parenchyma, an abundance of the unlabeled fibrillar sheath resulted in the enlargement of intercellular spaces (Fig. 2D). Fibrils and strands that constituted the extracellular sheath were closely associated

with host cell walls as well as with bacterial cells (Fig. 3A,B). In a more advanced stage, gold particles were detected over the fibrillar sheath close to host cells (Fig. 3C), or over portions of host walls detached from the main wall (Fig. 3C,D).

Five days after infection, bacteria colonized vessel cells (Fig. 4A). Examination of secondary walls of vessels and of the middle lamella showed that they could be severely damaged (Fig. 4B). Quantitation of gold particles indicated that labeling significantly decreased over primary walls of infected xylem cells (Table 1). The large standard errors of labeling density estimated on secondary walls indicated considerable variability in the degree of cell wall modification. Portions of host walls, enclosed in the extracellular sheath, showed weaker and uneven labeling (Fig. 4B). Sheath fibrils surrounding the pathogen were found to be closely asso-ciated with areas of degraded secondary vessel walls (Fig. 4B). Paramural appositions observed in periplasmic spaces of parenchymatous companion cells were at most weakly labeled (Figs. 4B and C).

At advanced stages of infection (4–12 days after inoculation), bacterial cells were typically localized in mesophyll intercellular spaces (Fig. 5A). Host cells displayed a strong electron-dense cytoplasm that could be detached from the cell wall (Fig. 5A). Numerous host cells were observed with collapsed cytoplasm. A significant reduction of labeling was also observed over walls of mesophyll cells (Table 1). Strands of material that occurred in the bacteria-surrounding sheath were closely associated with damaged walls (Fig. 5A).

**Labeling pattern of pectic substances observed in infected leaves.** A monoclonal antibody (JIM 5) raised against un-esterified epitopes of pectin was applied to infected leaves to analyze the pattern of pectin degradation in host cell walls. Examination of leaves showing colonized-substomatal cavities (48 h after infec-tion) revealed that the middle lamella had become disrupted in the vicinity of, or at a distance from, the pathogen (Figs. 5B and D). Quantitation of gold particles indicated that the labeling was markedly reduced over the middle lamella in the infected parenchyma tissue (Table 2). Altered areas of the milddle lamella were always found to be associated with the unlabeled sheath surrounding bacteria in which portions of labeled material were enclosed (Fig. 5C).

In the vascular stele, labeled paramural deposits were observed in phloem cells (Fig. 5E). Although bacterial cells colonized phloem elements only during the later stage of leaf collapse, middle lamella degradation seemed to occur frequently in this tissue as judged by the occurrence of gold particles in the lumen of sieve tubes (Fig. 6A). Disruption of the pit middle lamella and primary wall favored colonization of the vessel lumen (Fig. 6B–D). Multi-plication of bacteria in xylem cells was also accompanied by pronounced alteration of walls (Fig. 6B). Modification in the labeling pattern of the middle lamella (Table 2) indicated that pectin was altered in pit areas over which no, or few, gold particles were seen (Fig. 6C,D). The fibrillar sheath surrounding the pathogen in the lumen of vessels was always associated with degraded areas of walls and middle lamella (Figs. 6C,D, and 7A). The occurrence of an electron-dense material was noticed in vessels (Fig. 7B); the application of anti-pectin antibodies revealed the presence of gold particles over this dense material (Fig. 7C).

During the whole infection process, bacterial cells always showed an electron-dense cytoplasm (Figs. 2C, 4B, 6B) with few electron-lucent granules (Fig. 6B,D). The bacteria were always free of significant labeling after the use of the exoglucanase-gold complex and the anti-pectin antibodies. In contrast, numerous gold particles were seen over the material surrounding bacteria after incubation with anti-EPS antibodies (Fig. 7D) whereas no labeling occurred over plant cell elements.

## DISCUSSION

Major cytological studies on *Xanthomonas*-infected leaves have been conducted after wound inoculation (14,34,39), or infiltration of the mesophyll with a bacterial suspension (1,8,9,27,43). How-

ever, Bretschneider et al (7) and Wallis et al (48) infected cabbage leaves by the deposition of the inoculum on hydathodes, allowing a direct entrance of the pathogen into the protoxylem. Our observations, performed after spray inoculation of unwounded leaves, revealed that the pathogen entered through stomatal pores and subsequently colonized the lower mesophyll before entering the vascular stele. Since plant cell walls represent physical barriers to pathogen invasion, one may assume that they are likely to play an important role in this interaction. Previous work on *Xanthomonas*-infected plants mentioned that host walls were altered during the infection process (9,14,48). The present cytochemical investigation, dealing with subcellular localization of
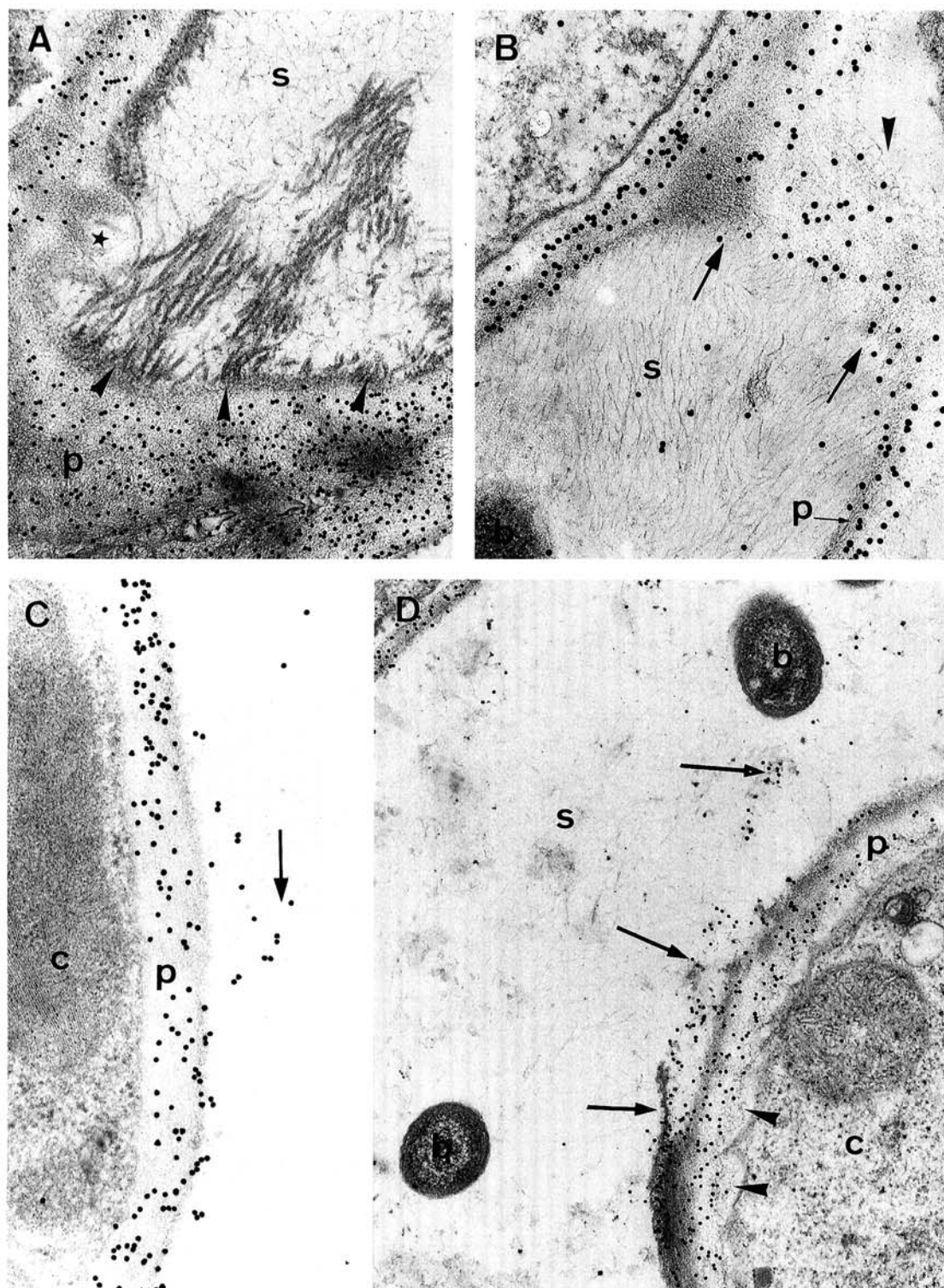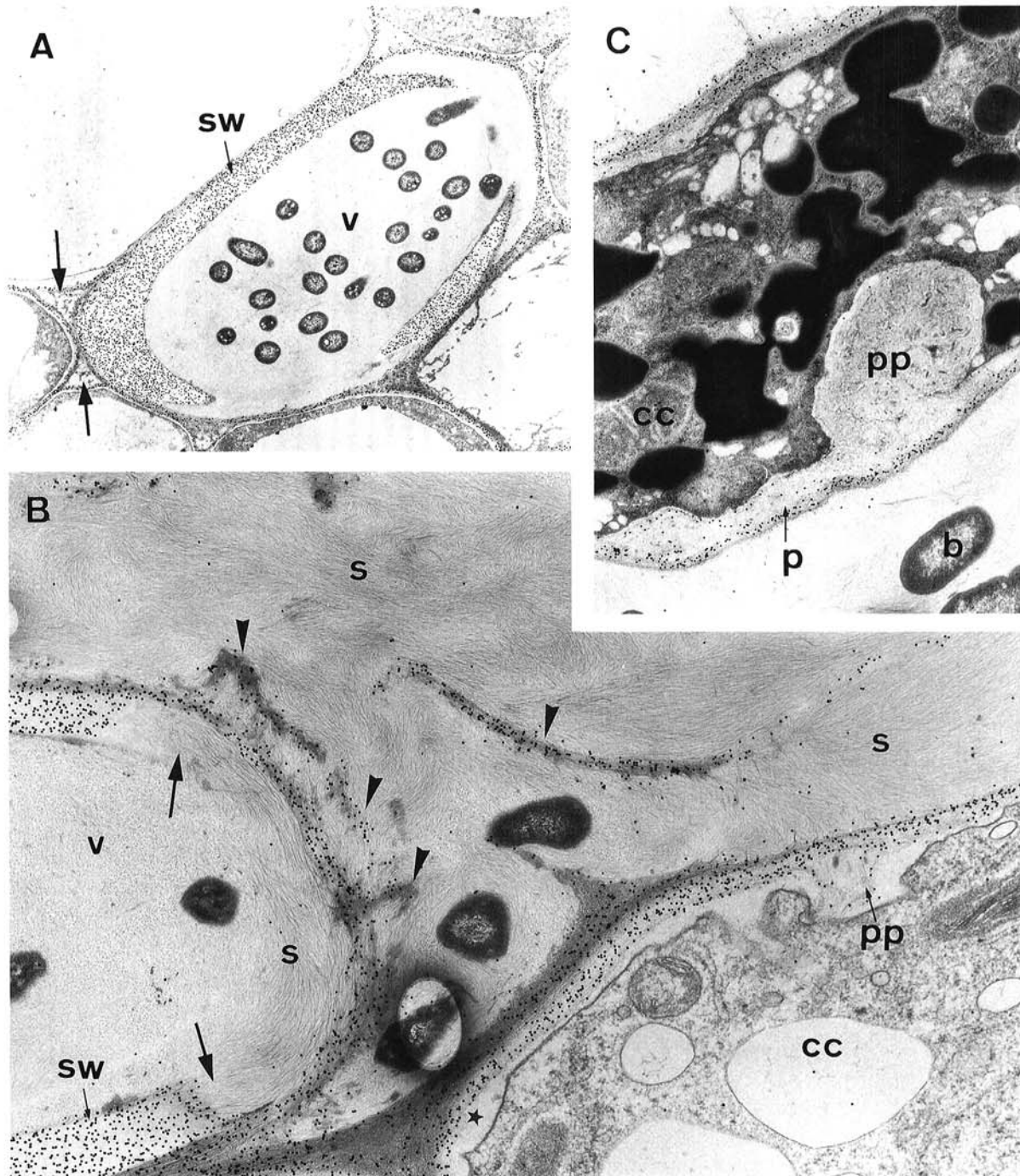


**Fig. 3. A–D,** TEM micrographs of infected cassava leaves by *Xanthomonas campestris* pv. *manihotis* fixed with glutaraldehyde and osmium tetroxide. Sections treated with exoglucanase-gold complex. **A,** 5 days after infection (dai), in mesophyll intercellular spaces, strands contained in fibrillar sheath (s) are in close contact (arrowheads) with primary host cell wall (p). Reduced labeling seen over portion of host wall (*). (×40,600). **B,** 5 dai, fibrils of surrounding-bacteria sheath (s) are in close contact (arrows) with the primary cell wall (p) of mesophyll cells. Few gold particles can be seen over sheath. Host cell displays portions of loosened wall (arrowhead). (×89,600). **C,** 3 dai, gold particles are present over fibrils (arrow) close to primary wall (p) of spongy parenchyma cell (c). (×64,800). **D,** 5 dai, the sheath (s) is associated with degraded areas of primary host cell wall (p). Uneven labeled fragments of host wall detached from main cell frame (arrows) can be observed within sheath. Few gold particles are seen over fibers in the periplasmic space (arrowheads) of the lower mesophyll cell (c). (×49,300).

galacturonic acid–containing molecules and β-1,4-glucans of infected leaf tissues, clearly demonstrated that cell walls are highly degraded in a susceptible cassava cultivar infected by *XCM*.

Discontinuity in the leaf cuticle layers between guard and subsidiary stomatal cell walls possibly favors pectin accessibility for and degradation by the pathogen. In such locations, bacterial colonies may survive on the leaf surface, but they were never seen to penetrate the leaf. During the whole infection process, host cell walls and middle lamellae displayed extensive disrupted areas regardless of the tissue colonized by *XCM* (intercellularly in the parenchyma, and intracellularly in xylem vessels and

tracheids). Variations in the labeling pattern of host cells are indicative of chemical modifications in walls, thus providing support for the importance of wall-degrading enzymes produced by *XCM* during pathogenesis on unwounded leaves. Dienelt and Lawson (14) also reported *Citrus* cell wall damages caused by *X. campestris* pv. *citri* on wound-inoculated detached leaves.

Although pathogenic species of *Xanthomonas* are not considered to be soft rotting bacteria, the production of pectinases in diseases caused by this pathogen (10,12,31) indicates that these enzymes may be locally required for host colonization during which intercellular substances are eroded. Our observation sup-



**Fig. 4. A–C,** TEM micrographs of cassava leaves infected by *Xanthomonas campestris* pv. *manihotis* fixed with glutaraldehyde and osmium tetroxide. Sections treated with exoglucanase-gold complex. **A,** 5 days after infection (dai), bacterial cells localized in lumen of vessel (v) in a vascular stele. The secondary cell wall (sw) is regularly labeled. Middle lamella (arrows) is degraded. (×9,000). **B,** 7 dai, cell wall and middle lamella degradation in a leaf vessel (v). The pathogen is present in intracellular and intercellular positions. The secondary cell wall (sw) shows highly degraded portions associated with the fibrillar bacteria-surrounding sheath (s) (arrows). Fragments of labeled host cell walls are located within the sheath (arrowheads). Cytoplasm of a companion cell (cc) is retracted (*) while unevenly labeled papilla (pp) occurs in periplasmic space. (×23,000). **C,** 7 dai, a globular papilla (pp) differentiated in periplasmic space of vessel companion cell (cc). Few gold particles are seen over this papilla, whereas host cell wall is evenly labeled (p). (×17,000).
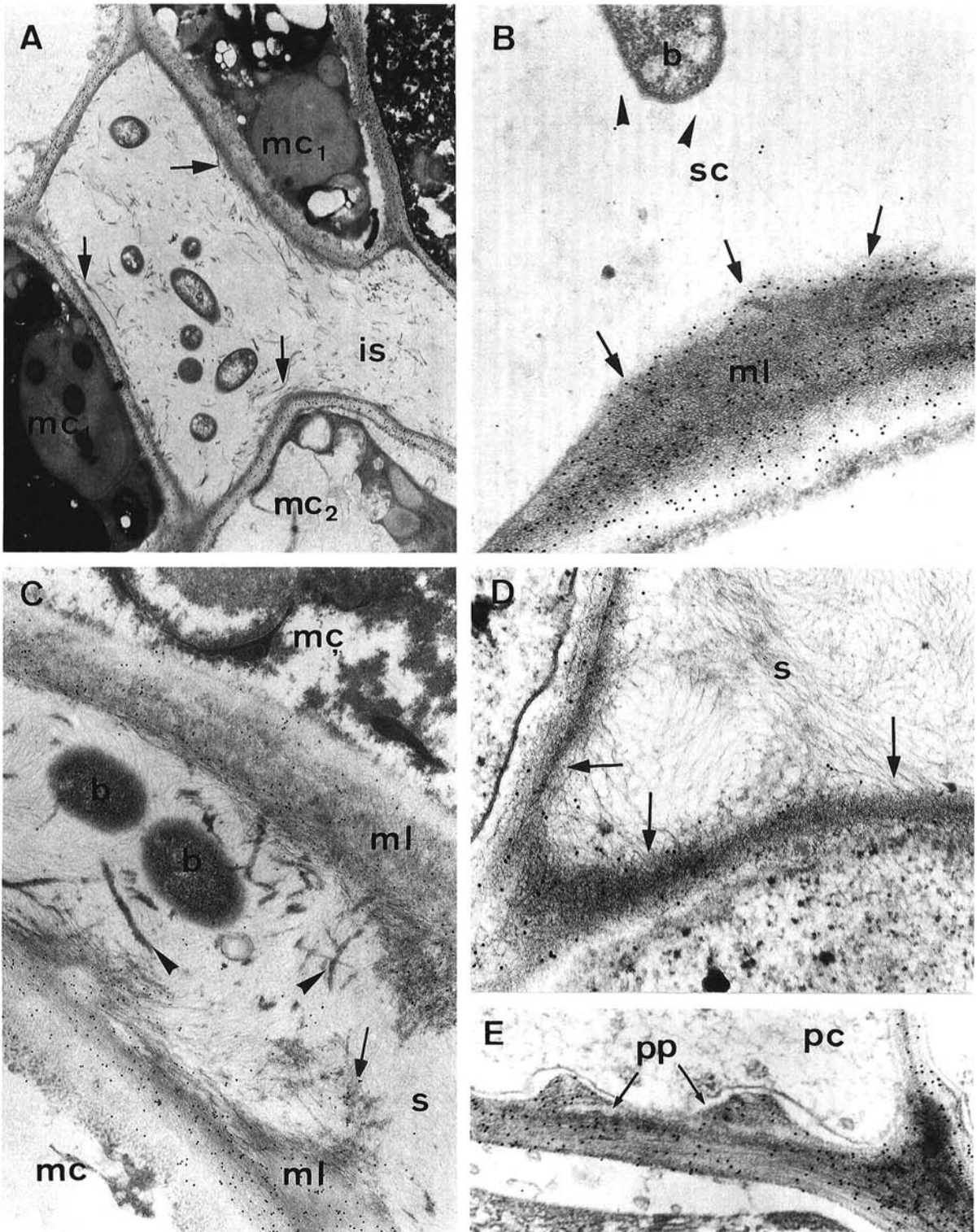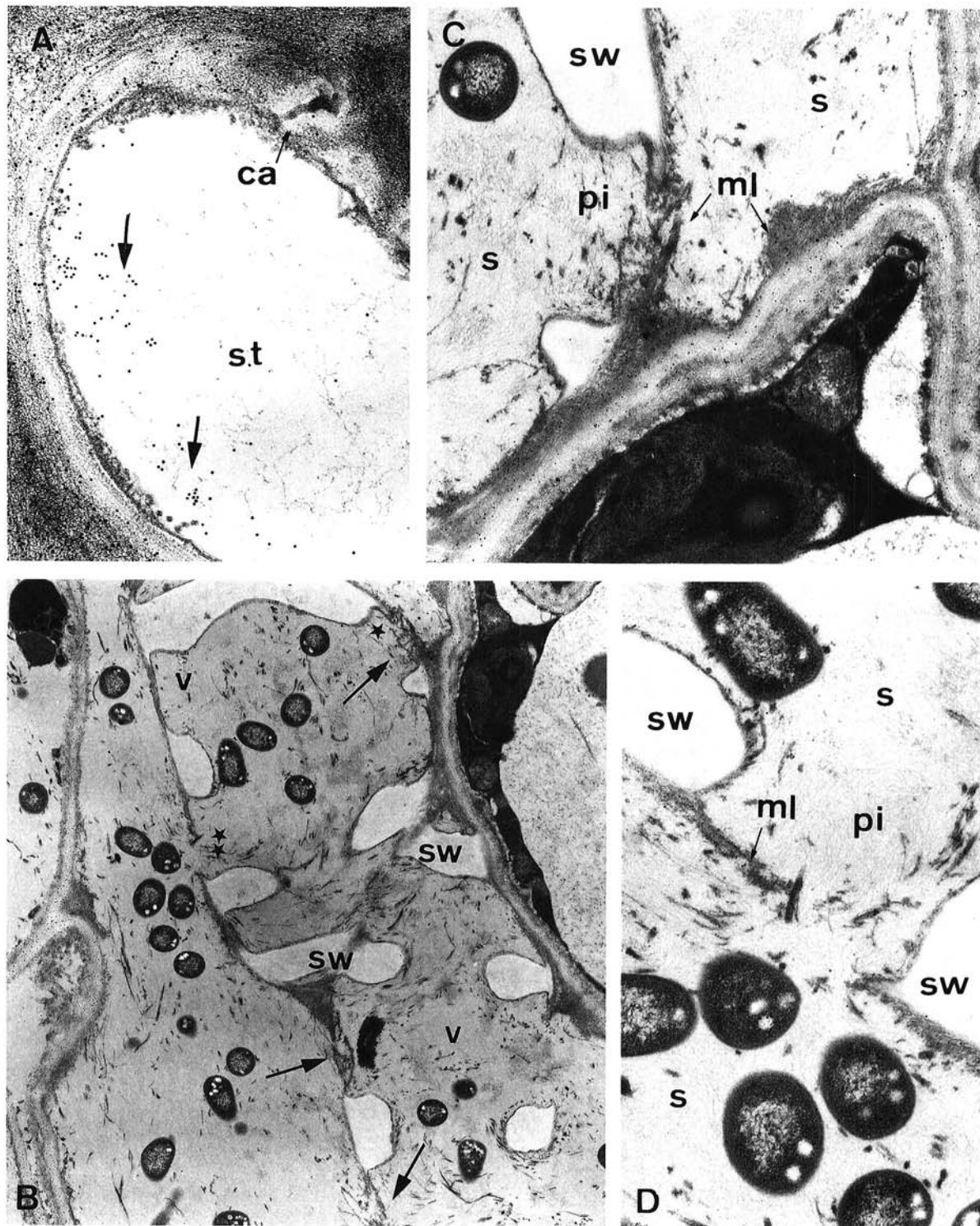
**Fig. 5. A–E,** TEM micrographs of infected cassava leaves infected by *Xanthomonas campestris* pv. *manihotis* fixed with glutaraldehyde and osmium tetroxide. **A,** 9 days after infection (dai), sections treated with exoglucanase-gold complex. Bacteria are localized in intercellular space (is) between mesophyll cells (mc) of leaf upper part. Strands of material within the extracellular sheath (arrows) are in close contact with the primary host cell wall. Two cells display an electron-dense cytoplasm (mc1); mc2 cell has collapsed. (×10000). **B–E,** Sections treated with JIM 5 anti-pectin antibodies. **B,** 2 dai, a bacterial cell (b) in a substomatal cavity (sc) shows unlabeled fibrils that arise from the pathogen (arrowheads). These fibrils are associated with a degraded portion of the labeled middle lamella (ml). At this site, loosened fragments of middle lamella are observed (arrows). (×52,200). **C,** 7 dai, two bacteria are present in middle lamella (ml) between two mesophyll cells (mc). Gold particles unevenly distributed over middle lamella, fragments of which are seen within sheath (arrow). Labeling is low over sheath (s) and strands associated with middle lamella (arrowheads). (×32,300). **D,** 2 dai, unlabeled fibrils of the extracellular sheath (s) are in close contact with the middle lamella (arrows), over which occur a few gold particles. (×64,800). **E,** 7 dai, two papillae (pp) are distinguishable in the periplasmic space of phloem cell (pc). Gold particles are seen over these papillae. (×6,000).

ports previous work performed in vitro on the occurrence of *XCM* polygalacturonase activity that was demonstrated by degradation of potato tuber slices (13). Although the role of pectinases in *XCM* pathogenicity remains unclear, they may actively contribute to bacterial progression in host tissue, and to plant necrosis by causing the loss of tissue cohesion. In this respect, it was found that pathogenicity of pleiotrophic *X. c.* pv. *campestris* mutants was restored by introduction of DNA with a polygalacturonase coding-sequence (12). However, among the three polygalacturonase lyase isozymes that were characterized, Dow et al (15) demonstrated that isozyme I was not absolutely necessary for pathogenesis.

Damage caused to cassava host middle lamellae is accompanied by the release of pectin oligomers as judged by gold particles interspersed within vessels and phloem cells, intercellular spaces,



**Fig. 6. A–D,** TEM micrographs of cassava leaves infected by *Xanthomonas campestris* pv. *manihotis* fixed with glutaraldehyde and osmium tetroxide, 7 days after infection (dai). Sections treated with JIM 5 anti-pectin antibodies. **A,** Gold particles (arrows) are scattered in the lumen of a phloem sieve tube (st). (ca = callose deposition). (×43,700). **B,** Localization of numerous bacterial cells in vascular stele results in pronounced alteration of vessel (v), cell walls (sw), and pits (arrows). Strands enclosed in the extracellular sheath are particularly abundant. Framed sections (*, **) are enlarged in Fig. 6C and D. (sw = secondary cell wall) (×9,600). **C,** Enlarged section of Fig. 6B*. Few gold particles are seen over pit (pi) middle lamella (ml). Sheath (s), associated with secondary cell wall (sw) is unlabeled. (×23,800). **D,** Enlarged section of Fig. 6B**. The unlabeled sheath (s) and strands of material associated with the degraded middle lamella (ml) of a pit (pi). Labeling is very low over this middle lamella. (×23,800).
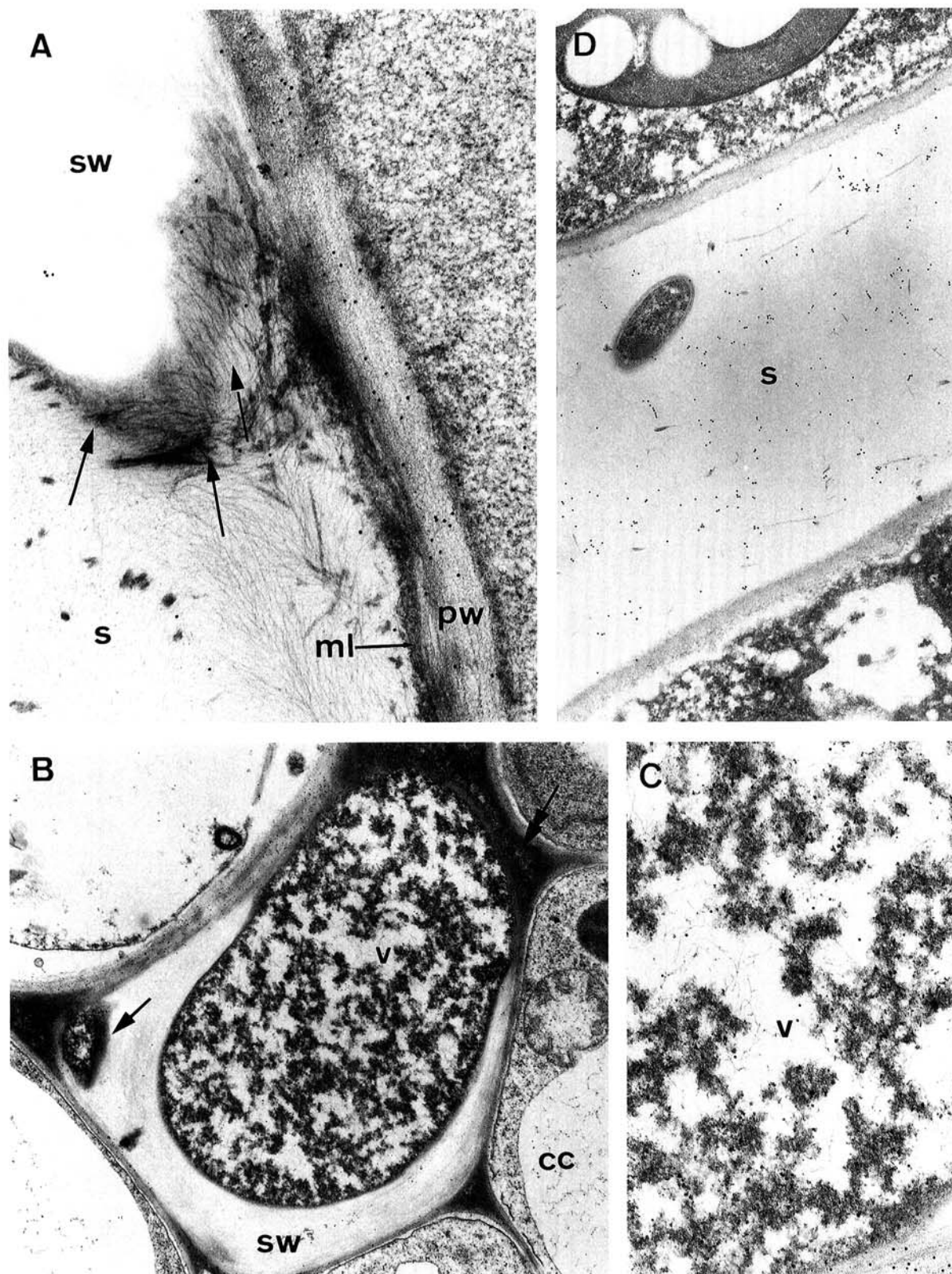
**Fig. 7. A–C,** TEM micrographs of infected cassava leaves by *Xanthomonas campestris* pv. *manihotis* fixed with glutaraldehyde and osmium tetroxide. Sections treated with JIM 5 anti-pectin antibodies. **A,** 7 days after infection (dai), the primary wall (pw) and middle lamella (ml) of a contact cell show low labeling. Unlabeled sheath fibrils (s) and sheath-enclosed strands are closely associated with degraded areas of the middle lamella and secondary cell wall (sw) (arrows). (×37,000). **B,** 9 dai, electron-dense material fills lumen of xylem vessel (v). Visible is the cavity in the secondary vessel wall (arrow) and degradation of the labeled middle lamella (doublearrow) (cc = companion cell). (×14,400). **C,** Enlargement of Fig. 7B. Gold particles associated with the electron-dense material fill vessel lumen. Unevenly labeled fibrils can also be seen in vessel (v). (×43,700). **D,** 5 dai, TEM micrographs of infected cassava leaves by *Xanthomonas campestris* pv. *manihotis* fixed with glutaraldehyde and paraformaldehyde. Sections treated with XB3 anti-EPS antibodies. Gold particles are distributed over material surrounding bacteria (s). No labeling is observed in the plant cell wall and cytoplasm. (×21,700).

and the material surrounding bacteria. Accumulation of pectin degradation compounds in vessels of cassava leaves could explain the occurrence of plugging material labeled with antipectin antibodies. It has been suggested that vessel plugs represent a host response in which released cell wall pectic components react with other host compounds (2). In cassava-infected leaves, wall appositions in vascular parenchyma cells constitute the only structural reaction we observed. Although polygalacturonic-containing molecules are known to be potent elicitors of plant defense (44), other structural and biochemical plant responses in our system need to be investigated.

Partial dissolution of host cell walls and the occurrence of labeled cell wall fragments in the fibrillar material surrounding bacteria also possibly resulted from the hydrolytic action of specific enzymes. Among plant bacterial pathogens, *Pseudomonas* (29), *Erwinia* (6), and *Clavibacter* (4) species are known to degrade cellulose and hemicellulose of plant cell walls (17). Ultrastructural evidence of primary cell wall degradation by *Xanthomonas* was reported for *X. c.* pv. *campestris*-infected cabbage leaves (48), for which wall shredding has been described. However, biochemical features indicating that enzymes of *Xanthomonas* are involved in wall polysaccharide degradation are poorly documented. A marked decrease in total cellulose was found in leaf tissues of *Citrus* infected by *X. c.* pv. *citri* (20). Similarly, a significant difference in cellulase activity was established in vitro for virulent and avirulent strains of *X. campestris* (31). It is also known that *X. c.* pv. *campestris* secretes an endoglucanase which has the potential capacity for degrading plant cell wall cellulose, but the role of this major extracellular protein in host-pathogen interaction remains obscure (12). In alfalfa infected with *X. c.* pv. *alfalfae,* the bacterial xylanase was demonstrated to play a causal role in pathogenesis (42); in this case, the decrease of plant xylan compounds was correlated with the increase of the bacterial xylanase activity. Although our study lacks biochemical data, this cytochemical investigation provides strong indirect evidence that *XCM* secretes active cellulases, or hemicellulases, or both, during leaf colonization.

Similarly, alteration of vessel cell walls and middle lamella in cassava leaves reveals that lignin-containing molecules are accessible to the pathogen during xylem invasion. It has been demonstrated in previous work that *Xanthomonas* depolymerizes lignin in vitro (17,30). Ultrastructural evidence of xylem secondary cell wall degradation by *Xanthomonas* was also reported elsewhere (24,48). These authors observed the accumulation of electron-opaque granules scattered in the invaded vessel lumina, which were interpreted as ligninlike components resulting from xylem cell wall swelling and shredding. Such granules were less abundant in the *XCM*-degraded xylem, but portions of cell walls were usually found in the sheath surrounding bacteria. In metaxylem cells, as also reported with *X. c.* pv. *campestris* (48), degradation of vessels by *XCM* mainly concerns the primary and the middle lamella, although extensive alteration of the secondary wall in advanced stages of the infection process was sometimes observed.

The accumulation of material surrounding *XCM* was observed from early colonization of the leaf surface to late infection of cassava leaves. This extracellular sheath is most likely to be of pathogen origin since a positive labeling was obtained with antibodies made to *Xanthomonas* EPS. Antibodies raised against an EPS-free strain of *XCM* did not yield any significant EPS labeling during the infection process (data not shown). The thick, unlabeled electron-dense strands occurring within the sheath during *XCM* infection process were similarly reported elsewhere in wheat leaves infected by *X. c.* pv. *undulosa* (18). These authors suggested that they originated in middle lamella shredding, although our investigation demonstrates that these strands were not labeled with anti-pectin antibodies. Strands in cassava leaves may result from synergistic interactions between xanthan and plant cell wall polysaccharides (36), modifications, if any, in charge, size, and viscosity of the xanthan polymer that could cause a local structural reorganization of the EPS (49), or the occurrence of plant cell compounds that are not targeted by the tested probes.

The functions of bacterial EPS in plant pathogenesis have been reviewed (35). Among the roles attributed to *Xanthomonas* EPS are contributions to water-soaking symptoms and to vascular occlusions, important factors in pathogenicity (40,41,46). It has been suggested that the toxicity of *XCM* EPS is not related to its effects on host cells (25). Since *XCM* EPS filled intercellular spaces, it was associated with degraded areas of cassava cell walls during the infection process. Also, EPS fibrils and strands were closely associated with detached portions of host cell walls, even surrounding them, likely providing a more accessible nutrient supply for the pathogen. In this compatible interaction between *XCM* and cassava, bacterial cells were seldom seen in close contact with the plant cell wall. Thus, the *XCM* extracellular sheath likely constitutes the main support for bacterial cell wall–degrading enzymes to reach plant substrate molecules. The accumulation of high amounts of cellulase found in vitro within EPS of *X. c.* pv. *glycines* supports this concept (23). It would be of interest to characterize cell wall–degrading enzymes during pathogenesis and to cytolocalize them as done elsewhere for fungal plant pathogens (38). In addition to being involved in plant cell wall degradation, *XCM* EPS may also protect the pathogen against toxicity of phenol-like molecules resulting from defense reactions or lignified cell wall degradation (17). If the bacterial cells are not able to detoxify their environment, then the extracellular sheath may function as an effective protective layer.

At the end of leaf colonization, large altered areas were visible within vascular bundles extending toward cortical tissues. These lysis pockets, in which numerous cells displayed degraded walls and cytoplasm (data not shown), enclosed both bacterial EPS and latex particles released by laticifer lysis. Latex from plants of the Euphorbiaceae family contains large amounts of cellulases involved in maturation of articulated laticifers (45). In this respect, the occurrence of laticifer-released cellulase in lysis pockets may contribute to the infection process by degrading leaf veins and the petiole, thus favoring bacterial egress and dissemination.

In conclusion, the present study provides new insights into cell wall degradation by *Xanthomonas* pathogens. Our results favor the hypothesis that lytic enzymes presumably of bacterial origin weaken and loosen the cell walls of cassava during host colonization by *XCM*. This cytochemical investigation indicates that pectic molecules are highly altered both in parenchyma cells and xylem vessels. Cellulose modification, as revealed by the reduction in labeling of $\beta$-1,4-glucans, is less in walls of xylem vessels than in walls of parenchyma cells. Whether such enzymes are required for pathogenicity remains unknown. To address this question, further studies are in progress to investigate wall alteration in a resistant cassava cultivar, compare cell wall degradation according to strain aggressiveness, and better understand the role of *XCM* EPS in wall degradation.

## LITERATURE CITED

1. Al-Mousawi, A. H., Richardson, P. E., Essenberg M., and Johnson, W. M. 1982. Ultrastructural studies of a compatible interaction between *Xanthomonas campestris* pv. *malvacearum* and cotton. Phytopathology 72:1222-1230.
2. Beckman, C. H. 1987. The nature of wilt diseases of plants. American Phytopathological Society, St. Paul, MN.
3. Benhamou, N. 1989. Cytochemical localization of $\beta$-(1-4)-D-glucans in plant and fungal cells using an exoglucanase-gold complex. Electron. Microsc. Rev. 2:123-138.
4. Benhamou, N. 1991. Cell surface interactions between tomato and *Clavibacter michiganense* subsp. *michiganense:* Localization of some poysaccharides and hydroxyproline rich glycoproteins in infected host leaf tissues. Physiol. Mol. Plant Pathol. 38:15-38.
5. Billing, E. 1987. Bacteria as plant pathogens. Pages 22-26 in: Aspects of Microbiology, vol. 14. E. Billing, ed. Van Nostrand Reinhold Co. Ltd., UK.
6. Braun, E. J., and Rodrigues, C. A. 1993. Purification and properties of an endoxylanase from a corn stalk rot strain of *Erwinia chrysanthemi.* Phytopathology 83:332-338.
7. Bretschneider, K. E., Gonella, M. P., and Robeson, D. J. 1989. A comparative light and electron microscopic study of compatible and incompatible interactions between *Xanthomonas campestris* pv.

*campestris* and cabbage (*Brassica oleracea*). Physiol. Mol. Plant Pathol. 34:285-297.

8. Brown, I., Mansfield, J., Irlam, I., Conrads-Strauch, J., and Bonas, U. 1993. Ultrastructure of interactions between *Xanthomonas campestris* pv. *vesicatoria* and pepper, including immunocytochemical localization of extracellular polysaccharides and the AvrBs3 protein. Mol. Plant-Microbe Interact. 6:376-386.

9. Cason, E. T., Jr., Richardson, P. E., Essenberg, M. K., Brinkerhoff, L. A., Johnson, W. M., and Venere, R. J. 1978. Ultrastructural cell wall alterations in immune cotton leaves inoculated with *Xanthomonas malvacearum*. Phytopathology 68:1015-1021.

10. Collmer, A., and Keen, N. T. 1986. The role of pectic enzymes in plant pathogenesis. Annu. Rev. Phytopathol. 24:283-409.

11. Daniel, J. F., and Boher, B. 1985. Epiphytic phase of *Xanthomonas campestris* pv. *manihotis* on aerial parts of cassava. Agronomie 5:111-116.

12. Daniels, M. J., Barber, C. E., Dow, J. M., Cough, C. L., Osbourn, A. E., and Tang, J. L. 1991. Molecular genetic dissection of pathogenicity of *Xanthomonas*. Pages 152-162 in: Biochemistry and Molecular Biology of Plant-Pathogen Interactions. C. J. Smith, ed. Clarendon Press, Oxford.

13. Dianese, J. C., and Dos Santos, L. T. P. 1985. Actividade pectolitica das patovares de *Xanthomonas campestris* que afetam a mandioca. Rev. Microbiol. 16:195-202.

14. Dienelt, M. M., and Lawson, R. H. 1989. Histopathology of *Xanthomonas campestris* pv. *citri* from Florida and Mexico in wound-inoculated detached leaves of *Citrus aurantifolia*: Transmission electron microscopy. Phytopathology 79:336-348.

15. Dow, J. M., Milligan, D. E., Jamieson, L., Barber, C. E., and Daniels, M. J. 1989. Molecular cloning of polygalacturonate lyase gene from *Xanthomonas campestris* pv. *campestris* and role of the gene product in pathogenicity. Physiol. Mol. Plant Pathol. 35:113-120.

16. Du Plessis, H. J. 1984. Scanning electron microscopy of *Xanthomonas campestris* pv. *pruni* in plum petioles and buds. Phytopathol. Z. 109:277-284.

17. Eriksson, K. E., Blanchette, R. A., and Ander, P. 1990. Microbial and Enzymatic Degradation of Wood and Wood Components. Springer Series in Wood Science. Springer Verlag, NY.

18. Ferauge, A. P., and Maraite, H. 1994. Light and electron microscopical study of the interactions between *Xanthomonas campestris* pv. *translucens* and pv. *undulosa* on wheat, barley and oat. Pages 813-818 in: Plant Pathogenic Bacteria. M. Lemattre, S. Freigoun, K. Rudolph, and J. G. Swings, eds. INRA/ORSTOM Editions, Paris.

19. Frens, G. 1973. Controlled nucleation for regulation of the particle size in monodisperse gold suspensions. Nature, Phys. Sc. 241:20-22.

20. Goto, M., and Okabe, N. 1959. Studies on the cellulolytic enzymes of phytopathogenic bacteria. Part 4. On the nature of cellulose in the lesions of black rot of cauliflower (*Xanthomonas campestris*) and *Citrus* canker (*Xanthomonas citri*). Rep. Fac. Agr. Shizuoka Univ. 9:21-23.

21. Gough, C. L., Dow, J. M., Barber, C. E., and Daniels, M. J. 1988. Cloning of two endoglucanase genes of *Xanthomonas campestris* pv. *campestris*: Analysis of the role of major endoglucanase in pathogenesis. Mol. Plant-Microbe Interact. 1:275-281.

22. Haaheim, L. R., Kleppe, G., and Sutherland, I. W. 1989. Monoclonal antibodies reacting with the exopolysaccharide xanthan from *Xanthomonas campestris*. J. Gen. Microbiol. 135:605-612.

23. Hokawat, S. 1988. Pathological characterization of the susceptible and resistant reaction of soybeans against the pathogen of pustule disease (*Xanthomonas campestris* pv. *glycines* Nakano, Dye). Ph.D. thesis. Göttingen, Germany.

24. Hüttermann, A. 1990. Electron microscopical studies of poplar clones inoculated with *Xanthomonas populi* subsp. *populi*. Eur. J. For. Pathol. 20:367-375.

25. Ikotun, T. 1984. The nature and function of the extracellular polysaccharide produced by *Xanthomonas campestris* pv. *manihotis*. Fitopatol. Bras. 9:467-473.

26. Ikotun, T. 1984. Inducible production of pectin-methylesterase by *Xanthomonas campestris* pv. *manihotis*. Z. Allg. Mikrobiol. 24:139-142.

27. Jones, S. B., and Fett, W. F. 1985. Fate of *Xanthomonas campestris* infiltrated into soybean leaves: An ultrastructural study. Phytopathology 75:733-741.

28. Kartha, K. K., and Gamborg, O. L. 1975. Elimination of cassava mosaic disease by meristem culture. Phytopathology 65:826-829.

29. Kelman, A., and Cowling, E. B. 1965. Cellulase of *Pseudomonas solanacearum* in relation to pathogenesis. Phytopathology 55:148-155.

30. Kern, H. W., and Kirk, T. K. 1987. Influence of molecular size and ligninase pretreatment on degradation of lignin by *Xanthomonas* sp. strain 99. Appl. Environ. Microbiol. 53:2242-2246.

31. Knösel, D., and Garber, E. D. 1967. Pektolitische une cellulolytische enzyme bei *Xanthomonas campestris* (Pammel) Dowson. Phytopathol. Z. 59:194-202.

32. Knox, J. P., Linstead, P. J., King, J., Cooper, C., and Roberts, K. 1990. Pectin esterification is spatially regulated both within cell walls and between developing tissues of root apices. Planta 181:512-521.

33. Koisumi, M. 1979. Ultrastructural changes in susceptible and resistant plants of *Citrus* following artificial inoculation with *Xanthomonas citri* (Hasse) Dowson. Ann. Phytopathol. Soc. Jpn. 45:635-644.

34. Lawson, R. H., Dienelt, M. M., and Civerolo, E. L. 1989. Histopathology of *Xanthomonas campestris* pv. *citri* from Florida and Mexico in wound-inoculated detached leaves of *Citrus aurantifolia*: Light and scanning electron microscopy. Phytopathology 79:329-335.

35. Leigh, J. A., and Coplin, D. C. 1992. Exopolysaccharides in plant-bacterial interactions. Annu. Rev. Microbiol. 46:307-346.

36. Morris, E. R., and Foster, T. J. 1994. Role of conformation in synergistic interactions of xanthan. Carbohydr. Polym. 23:133-135.

37. Nicole, M., and Benhamou, N. 1991. Cytochemical aspects of cellulose breakdown during the infection process of rubber tree roots infected by *Rigidoporus lignosus*. Phytopathology 81:1412-1420.

38. Nicole, M., Ruel, K., and Ouellette, G. B. 1994. Fine morphology of fungal structures involved in host cell wall alterations. Pages 13-31 in: Host Wall Alteration by Parasitic Fungi. O. Petrini and G. B. Ouellette, eds. American Phytopathological Society, St. Paul, MN.

39. Perreaux, D., Maraite, H., and Meyer, J. 1978. Histopathological study by fluorescent microscopy of cassava stems infected with *Xanthomonas manihotis*. Pages 395-398 in: Proc. Int. Conf. Plant Pathog. Bact., 4th. INRA, ed., Angers.

40. Pierce, M. L., Essenberg, M., and Mort, A. J. 1993. A comparison of the quantities of exopolysaccharide produced by *Xanthomonas campestris* pv. *malvearum* in susceptible and resistant cotton cotyledons during early stages of infection. Phytopathology 83:344-349.

41. Ramirez, M. E., Fucikovsky, L., Garcia-Jimenez, F., Quintero, R., and Galindo, R. 1988. Xanthan gum production by altered pathogenicity variants of *Xanthomonas campestris*. Appl. Microbiol. Biotechnol. 29:5-10.

42. Reddy, M. N., Stuteville, D. L., and Sorensen, E. L. 1974. Xylanase activity of *Xanthomonas alfalfae* in culture and during pathogenesis of bacterial leaf spot of alfalfa. Phytopathol. Z. 80:215-223.

43. Rudolph, K., Ebrahim-Nesbat, F., Mendgen, K., and Thiele, C. 1987. Cytological observations of leaf spot causing bacteria in susceptible and resistant hosts. Pages 604-612 in: Plant Pathogenic Bacteria. Proc. Int. Conf. Plant Pathog. Bact., 6th. E. L. Civerolo, A. Collmer, R. E. Davis, and A. G. Gillaspie, eds. Martinus Nijhoff Publishers, Dordrecht.

44. Ryan, C. A., and Farmer, E. E. 1991. Oligosaccharide signals in plants: A current assesment. Annu. Rev. Plant Phys. 42:651-674.

45. Sheldrake, A. R, and Moir, G. F. J. 1970. A cellulase in *Hevea* latex. Physiol. Plant. 23:267-277.

46. Sutton, J. C., and Williams, P. H. 1970. Relation of xylem plugging to black rot lesion development in cabbage. Can. J. Bot. 48:391-401.

47. Verdier, V., Schmit, J., and Lemattre, M. 1990. Etude en microscopie électronique à balayage de l'installation de deux souches de *Xanthomonas campestris* pv. *manihotis* sur feuilles de vitroplants de manioc. Agronomie 2:93-102.

48. Wallis, F. M., Rijkenberg, F. H. J., Joubert, J. J., and Martin, M. M. 1973. Ultrastructural histopathology of cabbage leaves inoculated with *Xanthomonas campestris*. Physiol. Plant Pathol. 3:371-378.

49. Zhan, D. F., Ridout, M. J., Brownsey, G. J., and Morris V. J. 1993. Xanthan-locus bean gum interactions and gelation. Carbohydr. Polym. 21:53-58.